1521-0103/345/2/189–197$25.00
THE JOURNAL OF PHARMACOLOGY AND EXPERIMENTAL THERAPEUTICS

http://dx.doi.org/10.1124/jpet.112.201046
J Pharmacol Exp Ther 345:189–197, May 2013

Novel Insights into CB_1 Cannabinoid Receptor Signaling: A Key Interaction Identified between the Extracellular-3 Loop and Transmembrane Helix 2[S]

Jahan Marcu, Derek M. Shore, Ankur Kapur, Megan Trznadel, Alexandros Makriyannis, Patricia H. Reggio, and Mary E. Abood

Department of Anatomy and Cell Biology and Center for Substance Abuse Research, Temple University, Philadelphia, Pennsylvania (J.M., A.K., M.T., M.E.A.); Center for Drug Discovery, University of North Carolina at Greensboro, Greensboro, North Carolina (D.M.S., P.H.R.); and Center for Drug Discovery, Northeastern University, Boston, Massachusetts (A.M.)

Received October 22, 2012; accepted February 19, 2013

ABSTRACT

Activation of the cannabinoid CB_1 receptor (CB_1) is modulated by aspartate residue D2.63[176] in transmembrane helix (TMH) 2. Interestingly, D2.63 does not affect the affinity for ligand binding at the CB_1 receptor. Studies in class A G protein-coupled receptors have suggested an ionic interaction between residues of TMH2 and 7. In this report, modeling studies identified residue K373 in the extracellular-3 (EC-3) loop in charged interactions with D2.63. We investigated this possibility by performing reciprocal mutations and biochemical studies. D2.63[176]A, K373A, D2.63[176]A-K373A, and the reciprocal mutant with the interacting residues juxtaposed D2.63[176]K-K373D were characterized using radioligand binding and guanosine 5′-3-*O*-(thio) triphosphate functional assays. None of the mutations resulted in a significant change in the binding affinity of *N*-(piperidiny-1-yl)-5-(4-chlorophenyl)-1-(2,4-dichloro-phenyl)-4-methyl-1*H*-pyrazole-3-carboxamide hydrochloride (SR141716A) or (−)-*3cis* -[2-hydroxyl-4-(1,1-dimethyl-heptyl)phenyl]-*trans*-4-[3-hydroxyl-propyl] cyclohexan-1-ol (CP55,940). Modeling studies indicated that binding-site interactions and energies of interaction for CP55,940 were similar between wild-type and mutant receptors. However, the signaling of CP55,940, and *(R)*-(+)-[2,3-dihydro-5-methyl-3-[(4-morpholinyl)methyl]-pyrrolo[1,2,3-*de*]-1,4-benzoxazin-6-yl](1-naphthalenyl)-methanone mesylate (WIN55,212-2) was impaired at the D2.63[176]A-K373A and the single-alanine mutants. In contrast, the reciprocal D2.63[176]K-K373D mutant regained function for both CP55,940 and WIN55,212-2. Computational results indicate that the D2.63[176]-K373 ionic interaction strongly influences the conformation(s) of the EC-3 loop, providing a structure-based rationale for the importance of the EC-3 loop to signal transduction in CB_1. The putative ionic interaction results in the EC-3 loop pulling over the top (extracellular side) of the receptor; this EC-3 loop conformation may serve protective and mechanistic roles. These results suggest that the ionic interaction between D2.63[176] and K373 is important for CB_1 signal transduction.

Introduction

The cannabinoid CB_1 receptor (CB_1), a member of the class A rhodopsin-like family of G protein-coupled receptors (GPCRs) (see Fig. 1), is found primarily in the central nervous system (CNS) and is important in the regulation of neuronal activity. In addition, there is evidence that the CB_1 receptor is expressed in peripheral tissues (albeit to a lesser extent), including the adrenal gland, bone marrow, heart, lung, and prostate (Howlett et al., 2002). The CB_1 receptor, a Gi/o coupled GPCR binds five structurally diverse classes of ligands; these include the endocannabinoids (typified by anandamide and 2-arachidonoylglycerol), the classic and nonclassic cannabinoids (typified by δ-9-tetrahydrocannabinol and CP55,940 [(−)-*cis*-3-[2-hydroxyl-4-(1,1-dimethylheptyl) phenyl]-*trans*-4-[3-hydroxyl-propyl] cyclohexan-1-ol], respectively), the aminoalkylindoles (typified by WIN55,212-2 [*(R)*-(+)-[2,3-dihydro-5-methyl-3-[(4-morpholinyl)methyl]-pyrrolo [1,2,3-*de*]-1,4-benzoxazin-6-yl](1-naphthalenyl)methanone mesylate]), and the diarylpyrazole antagonists/inverse agonists [typified by SR141716A (*N*-(piperidiny-1-yl)-5-(4-chlorophenyl)-1-(2,4-dichlorophenyl)-4-methyl-1*H*-pyrazole-3-carboxamide hydrochloride)] (see Fig. 2) (Picone et al., 2002).

Considering its fundamental role in the CNS, it is not surprising that the CB_1 receptor has been reported to mitigate numerous pathologies, including Alzheimer's disease, cancer, obesity, and pain (Pertwee, 2009). Unfortunately, many attempts

This work was supported by the National Institutes of Health National Institute on Drug Abuse [Grants DA003934, DA021358, DA023204, and DA09158].
dx.doi.org/10.1124/jpet.112.201046.
[S] This article has supplemental material available at jpet.aspetjournals.org.

ABBREVIATIONS: B_{max}, maximal binding; CB_1, cannabinoid CB_1 receptor; CL, confidence limit; CP55,940, (−)-*cis*-3-[2-hydroxyl-4-(1,1-dimethylheptyl)phenyl]-*trans*-4-[3-hydroxyl-propyl] cyclohexan-1-ol; EC, extracellular loop; E_{max}, maximal effective response; GPCRs, G protein-coupled receptors; GTPγS, guanosine 5′-3-*O*-(thio)triphosphate; HEK, human embryonic kidney; IC loop, intracellular loop; K_d, equilibrium dissociation constant; K_i, inhibitory constant; SR141716A, *N*-(piperidiny-1-yl)-5-(4-chlorophenyl)-1-(2,4-dichlorophenyl)-4-methyl-1*H*-pyrazole-3-carboxamide hydrochloride; TMH, transmembrane helices; WIN55,212-2,*(R)*-(+)-[2,3-dihydro-5-methyl-3-[(4-morpholinyl)methyl]-pyrrolo[1,2,3-*de*]-1,4-benzoxazin-6-yl](1-naphthalenyl)methanone mesylate; WT, wild type.

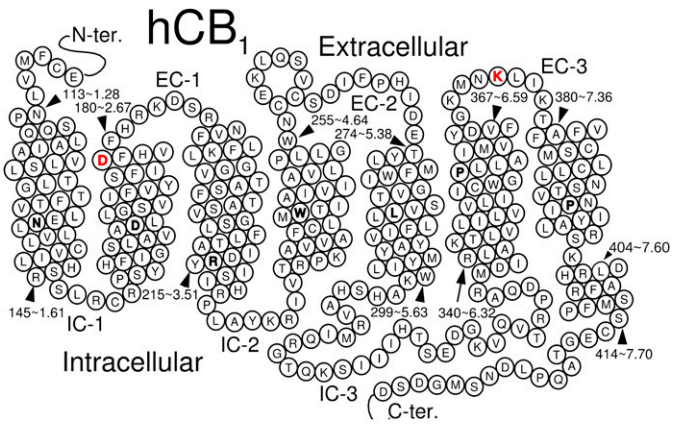

Fig. 1. Helix net representation of the hCB_1 receptor sequence. The most highly conserved residue position in each transmembrane helix across class A GPCRs is highlighted in bold. The amino acids mutated in this study are highlighted in red.

at harnessing the therapeutic potential of the CB_1 receptor have failed due to unacceptable CNS-related side effects, such as euphoria, depression, and suicidal fixation (Christopoulou and Kiortsis, 2011). Clearly, a better understanding of the CB_1 receptor's signal transduction mechanism(s) at a molecular level would be useful in realizing this receptor's therapeutic potential.

Traditionally, the high degree of sequence homology of amino acid residues from transmembrane helices (TMHs) of different GPCRs has led to the identification of conserved residues, which have been shown to be crucial for receptor function using biochemical studies (Tao and Abood 1998). In addition, charged interactions between amino acid residues from different TMH domains have been shown to be essential for either ligand binding or receptor function (Zhou et al., 1994; Sealfon et al., 1995; Xu et al., 1999). Residues from the extracellular (EC) loops demonstrate low sequence homology (Peeters et al., 2011b) and were initially thought to connect the TMH domains rather than to have a direct role in receptor functioning.

However, recent studies have demonstrated the critical role of the EC loops to ligand binding and receptor signaling. Mutation studies have demonstrated that the first EC loop (EC-1 loop) is important to the activation of the adenosine A_{2B} receptor (Peeters et al., 2011a). The second EC loop (EC-2 loop) has been shown to be important in ligand binding and activation at the V_{1a} vasopressin receptor (Conner et al., 2007), to be important to helix movement in rhodopsin (Ahuja et al., 2009), and to be involved in the binding of allosteric modulators at the M_2 acetylcholine receptor (Avlani et al., 2007). Less is known about the third EC loop (EC-3 loop); however, a key salt bridge between the EC-3 and EC-2 loops has been observed to influence ligand binding and receptor activation at the β_2-adrenergic receptor (Bokoch et al., 2010).

The EC-1 and EC-2 loops of the CB_1 receptor (Murphy and Kendall, 2003; Ahn et al., 2009a; Bertalovitz et al., 2010) have been better characterized than its EC-3 loop. EC-3 loop modeling studies reported here suggest that the EC-3 loop residue K373 may form a functionally-important ionic interaction with a transmembrane residue, $D2.63^{176}$. Our previous $D2.63^{176}$ mutation studies have demonstrated that the negative charge of $D2.63^{176}$ is critical for agonist efficacy but not ligand binding at the CB_1 receptor (Kapur et al., 2008). We hypothesized that this functional requirement (of a negatively charged residue at 2.63^{176}) may be due to this residue's participation in an ionic interaction with K373 that is necessary for signal transduction. To test this hypothesis, three mutations that would disrupt this putative interaction, $D2.63^{176}$A, K373A, and $D2.63^{176}$A-K373A, and a charge-reversal mutation $D2.63^{176}$K-K373D that would restore the interaction were evaluated for their impact on ligand binding and agonist efficacy. The binding affinities for CP55,940 and SR141716A were not significantly affected by any of the mutations. However, the efficacy of CP55,940 and WIN55,212-2 was markedly reduced by the alanine-substitution mutations, while the charge-reversal mutation led to partial rescue of wild-type (WT) levels of efficacy. Computational results indicate that the $D2.63^{176}$-K373 ionic interaction strongly influences the conformation(s) of the EC-3 loop, providing a structure-based rationale for the importance of the EC-3 loop to signal transduction in CB_1. Specifically, the putative ionic interaction results in the EC-3 loop pulling over the top (EC side) of the receptor; this EC-3 loop conformation may serve protective and mechanistic roles.

Our results have for the first time identified an interaction between the residues from TMH2-EC3, suggesting the proximity of these two domains and their role in modulating CB_1 signal transduction.

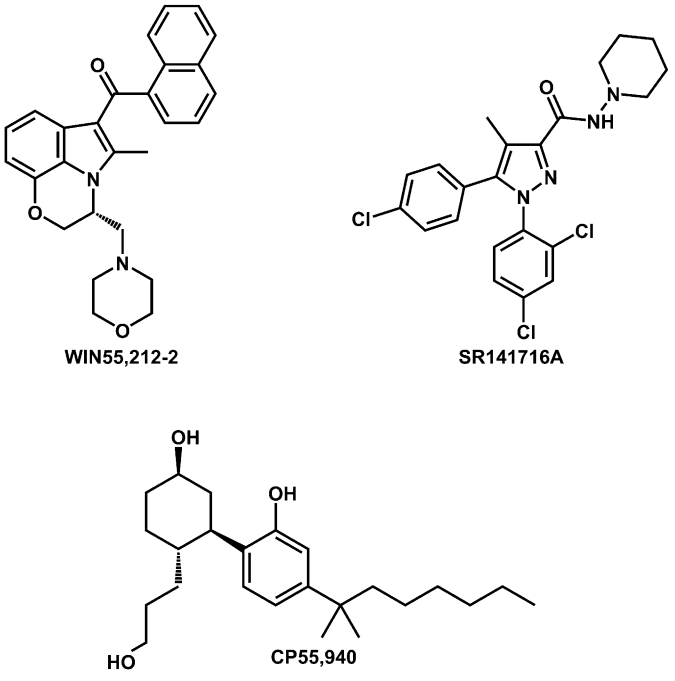

Fig. 2. Compounds evaluated in this study.

Materials and Methods

Materials

[^{3}H]CP55,940 (160-180 Ci/mmol) and [^{35}S]GTPγS (guanosine 5′-3-*O*-(thio)triphosphate; 1250 Ci/mmol) were purchased from PerkinElmer (Boston, MA). WIN55,212-2, CP55,940, and SR141716A were obtained from Tocris (Ellisville, MI). The *Pfu* Turbo DNA polymerase for mutagenesis experiments was from Stratagene (La Jolla, CA). All

other reagents were obtained from Sigma-Aldrich (St. Louis, MO) or other standard sources. The CB_1 antibody was kindly provided by Ken Mackie (Indiana University).

Amino Acid Numbering

The numbering scheme suggested by Ballesteros and Weinstein (1995) was employed here. In this system, the most highly conserved residue in each TMH is assigned a locant of 0.50. This number is preceded by the TMH number and followed by the absolute sequence number in superscript. All other residues in a TMH are numbered relative to this residue. The sequence numbers used are human CB_1 sequence numbers unless otherwise noted (Bramblett et al., 1995).

Mutagenesis and Cell Culture

The D2.63^{176}A, K373A, D2.63^{176}A-K373A, and D2.63^{176}K-K373D mutants of the human CB_1 in the vector pcDNA3 were constructed using the QuikChange site-directed mutagenesis kit (Stratagene). The mutagenic oligonucleotides used were between 27 and 33 base pairs long. Restriction endonuclease digestion and DNA sequencing subsequently confirmed the presence of the mutation. Stably transfected human embryonic kidney (HEK)-293 cell lines were created by transfection with WT or mutant CB_1-pcDNA3 cDNA by the lipofectamine reagent (Invitrogen, Carlsbad, CA) and selected in growth medium containing geneticin (1 mg/ml), as previously described elsewhere (McAllister et al., 2003).

Radioligand Binding and GTPγS Binding Assay

Protein membrane preparations harvested from stably transfected HEK293 cells were prepared and assayed as previously described elsewhere (Kapur et al., 2007). In brief, binding assays (saturation and competition binding assays) were initiated by the addition of 50 μg membrane protein to glass tubes pretreated with siliconizing fluid (Pierce, Rockford, IL; to reduce nonspecific binding) containing [^{3}H]SR141716A, and an appropriate volume of binding buffer A (50 mM Tris-Base, 1 mM EDTA, 3 mM $MgCl_2$, and 5 mg/ml bovine serum albumin, pH7.4) to bring the final volume to 500 μl. Nonspecific binding was determined in presence of excess (1 μM) unlabeled SR141716A. Reactants were allowed to reach equilibrium (~1 hour). Subsequently, free and bound radioligand were separated by vacuum filtration through Whatman GF-C filters, and the radioactivity retained on the filters was quantified by a liquid scintillation counter.

The K_d (equilibrium dissociation constant) and B_{max} (maximal binding) values were determined by analyzing the saturation binding data by nonlinear regression and fitted to a one-site binding model using GraphPad Prism 4.0 software (GraphPad, San Diego, CA). The displacement log IC_{50} values were determined by nonlinear regression and fitting the data to one-site competition and then were converted to K_i (inhibitory constant) values using the Cheng and Prusoff method (Cheng and Prusoff, 1973) with the use of GraphPad Prism.

The GTPγS assay was initiated by the addition of 20 μg of membrane protein into silanized glass tubes containing 0.1 nM [^{35}S]GTPγS, 10 μM GDP in GTPγS binding buffer (50 mM Tris-HCl, 100 mM NaCl, 3 mM $MgCl_2$, 0.2 mM EGTA, and 0.1% bovine serum albumin, pH7.4). Nonspecific binding was assessed in the presence of 20 μM unlabeled GTPγS. Free and bound radioligand were separated, and bound radioactivity was quantified as described previously. Nonlinear regression of log concentration values versus the percentage effect fitted to sigmoidal dose-response was used to obtain estimates of agonist concentrations that elicit half the maximal response (EC_{50}) and maximal response (E_{max}).

Statistical Analyses

Data are reported as the mean value of the replicates along with their 95% confidence limits (CL). The K_i and log EC_{50} values in the mutant and WT CB_1 receptors were compared using one-way analysis of variance with Bonferroni multiple comparison post tests. $P<.05$ was considered statistically significant.

Molecular Modeling

Receptor Model Construction Protocol for Loop Calculations. *Wild-type CB_1 activated (R*) receptor model construction.* Using interactive computer graphics, extracellular (EC-1 F180–S185, EC-2 G254–E273, and EC-3 G369–K376) and intracellular loops (IC-1 R145–R150, IC-2 P221–T229, and IC-3 S303–M336) were manually added to our previously constructed TMH bundle model of the CB_1 R* (active state) receptor, with CP55,940 docked in its global minimum energy conformation (Kapur et al., 2007). The program Modeler was then used to refine loop structures (Sali and Blundell, 1993; Fiser et al., 2000). Because of their close spatial proximity, the conformations of all three EC loops were calculated together followed by calculation of the three IC loop conformations. Chosen loop conformations were those that produced a low value of the Modeler objective function. The loops were minimized in three stages (stages 1 to 3, as described later). Next, portions of the N and C termini were added, and conformations of each were refined in Modeler. The termini were minimized using stages 4 to 5 of the minimization protocol.

N terminus. The first 89 residues of the N terminus were truncated, based on results from the Chin laboratory (Andersson et al., 2003) which showed that CP55,950 has WT binding affinity and efficacy at the N-terminal truncated CB_1, whereas the receptor has better cell surface expression than WT. X-ray crystal structures of class A GPCRs with lipid-derived endogenous ligands show that the N terminus occludes the binding pocket. In the crystal structure of rhodopsin (Li et al., 2004), the N terminus is positioned centrally, occluding the EC side of the bundle (i.e., the retinal plug). This general placement of the N terminus is also observed in the crystal structure of the sphingosine 1-phosphate receptor (Hanson et al., 2012). Because CB_1 also has a lipid-derived endogenous ligand, a truncated N-terminal conformation (positioned centrally over the EC side of the receptor) was chosen.

EC-2 loop. One of the significant sequence divergences between rhodopsin and CB_1 is in the EC-2 loop region. This loop in CB_1 is shorter than in rhodopsin and is missing the conserved disulfide bridge between the cysteine in the EC-2 loop and C3.25 in TMH3 of rhodopsin. Instead, there is a Cys at the extracellular end of TMH4 in CB_1 and a Cys near the middle of the EC-2 loop that experiments suggest may form a disulfide bridge (Fay et al., 2005). Consequently, the position of the EC-2 loop with respect to the binding site crevice in CB_1 around TMHs 3, 4, and 5 is likely to be quite different from that in rhodopsin. Therefore, this loop was modeled with an internal C257–C264 disulfide bridge based upon mutation results from the Farrens laboratory (Fay et al., 2005), which show that these two cysteines are required for high-level expression and receptor function.

To guide selection of an appropriate EC-2 loop conformation, we used mutation results from the Kendall laboratory (Ahn et al., 2009a; Bertalovitz et al., 2010), which demonstrate that mutation of EC-2 loop residue F268 to a tryptophan severely damages the binding affinity and efficacy of CP55,940 but has no significant effect on the binding affinity of SR141716A. Thus, an EC-2 loop conformation was chosen that placed F268 in close proximity to CP55,940. A F268W mutant bundle was constructed to verify that this mutation resulted in significant steric overlaps with CP55,940 in our model but not with SR141716A (Supplemental Fig. 1).

EC-3 loop. The EC loops were refined by use of Modeler in two stages. In the first stage, no harmonic distance constraints were used. This calculation was performed to examine the general conformational space of the EC-3 loop. The EC-3 loop conformation with the lowest objective function placed the EC-3 loop over the top of the receptor; in addition, the putative ionic interaction between D2.63^{176}

and K373 had formed. In the second stage, a 3.0 kcal/mol harmonic distance constraint was placed between the EC-3 loop residue K373 and D2.63^{176}. Specifically, the distance between the OD1 atom of D2.63^{176} and the NZ atom of K373 was constrained to 3.0 ± 2.0 Å. This second calculation was performed to obtain a focused conformational sampling of the EC-3 loop conformation with the lowest objective function (obtained in the first stage of the calculation).

IC-3 loop. The CB_1 IC-3 loop is much longer than the corresponding sequence in rhodopsin. Nuclear magnetic resonance experiments have been performed on a peptide fragment composed of the CB_1 sequence span from the IC end of TMH5 to the IC end of TMH6 in micelles (Ulfers et al., 2002). This study suggested that part of the IC-3 loop is α helical. This region occurs after the IC end of TMH5 [K5.64^{300}] and consists of a short α-helical segment from A301 to R307, followed by an elbow region (R307–I309) and an α-helical segment (Q310–S316) up to an III sequence (I317–I319) in IC-3. Based on these results, we replaced the initial Modeler-built IC-3 loop with this α-helix-elbow-α-helix region, and then the rest of IC-3 loop (I317–P332) was rebuilt and optimized using Modeler.

C terminus. A C-terminal fragment S414–G417, which contains a putative palmitoylation site at Cys^{415} (Fay et al., 2005), was added to the model and C415 was palmitoylated. C-terminal truncation experiments from the Mackie laboratory (Jin et al., 1999) have shown that CB_1 (with truncation at C417) signals normally in the presence of agonists. With the exception of helix 8, the C terminus is largely unstructured, though recent work on an isolated C-terminal peptide suggests the existence of an additional C-terminal helix, helix 9 (Ahn et al., 2009b). However, recent results from the Mackie laboratory (Straiker et al., 2012) reinforce that the functional significance of the C terminus pertains to desensitization and receptor internalization—not necessarily to receptor signaling by heterotrimeric G proteins. Therefore, we modeled the truncated C terminus as unstructured.

Receptor Model Energy Minimization Protocol. The energy of the ligand/CB_1 R* complex, including loop regions and N and C termini, was minimized using the OPLS 2005 force field in Macromodel 9.9 (Schrödinger Inc., Portland, OR). An 8.0-Å extended nonbonded cutoff (updated every 10 steps), a 20.0-Å electrostatic cutoff, and a 4.0-Å hydrogen bond cutoff were used in each stage of the calculation.

The minimization was performed in five stages. In the first stage of the calculation, the ligand and TMH bundle were frozen, but the loops were allowed to relax. The generalized born/surface area continuum solvation model for water as implemented in Macromodel was used. This stage of the calculation consisted a of Polak–Ribier conjugate gradient minimization in 1000-step increments until the bundle reached the 0.05 kJ/mol gradient. Because mutation results from the Kendall laboratory (Ahn et al., 2009a; Bertalovitz et al., 2010) demonstrate that mutation of EC-2 loop residue F268 to a tryptophan severely damages the binding affinity and efficacy of CP55,940, the terminal side-chain hydrogen of F268 (atom name: HZ) was frozen in place. Freezing this hydrogen allowed F268 the most conformational freedom, allowing the side-chain to pivot about HZ while requiring F268 to stay in close proximity to CP55,940. The second stage of the calculation was performed exactly as the first stage, except that HZ of F268 was unfrozen.

In the third stage, the loops were frozen but the ligand and the side chains of the TMHs were allowed to optimize. The minimization consisted of a conjugate gradient minimization using a distance-dependent dielectric, performed in 1000-step increments until the bundle reached the 0.05 kJ/mol gradient. Because a previously minimized TMH bundle was used as the starting structure in constructing this model (Kapur et al., 2007), the backbone atoms of the transmembrane helices were frozen to prevent the bundle from over packing.

In the fourth stage, the N and C termini were minimized using the same protocol used in second stage. In this stage, only the termini were minimized. In the fifth stage, the TMH bundle was minimized again, exactly as described in the third stage.

Mutant CB_1 activated (R) receptor models construction and minimization.* Four mutant bundles were constructed: K373A, D2.63^{176}A, D2.63^{176}A-K373A, and D2.63^{176}K-K373D. These mutant models were constructed using the final WT CB_1 R* model (Kapur et al., 2007) as the starting structure, using interactive computer graphics to perform the appropriate mutations. The N terminus was temporarily removed to prevent it from biasing the mutant loop refinement. Modeler was used (as before) to refine the EC-1 and EC-3 mutant loop structures. No harmonic distance constraint was used for the alanine-substitution mutants (however, the same distance constraint used for WT was also used for D2.63^{176}K-K373D).

The WT conformations of the EC-2 loop, the IC loops, and the termini were preserved. As with the WT CB_1 R*, the chosen loop configurations for the mutant bundles were those that produced a low value of the Modeler objective function; the loops were minimized using stages 1 to 3 of the minimization protocol (see above). Next, the N terminus was reattached to the mutant bundles. The termini were minimized using stages 4 to 5 of the minimization protocol (see the earlier description).

Assessment of Pairwise Interaction and Total Energies

Interaction energies between CP55,940 and the WT, K373A, D2.63^{176}A, D2.63^{176}A-K373A, or D2.63^{176}K-K373D receptors were calculated using Macromodel (Schrodinger). After defining the atoms of CP55,940 as one group (group 1) and the atoms corresponding to a residue that lines the binding site in the final ligand/CB1 R* complex as another group (group 2), Macromodel was used to output the pairwise interaction energy (coulombic and van der Waals) for a given pair of atoms. The pairs corresponding to group 1 (ligand) and group 2 (residue of interest) were then summed to yield the interaction energy between the ligand and the receptor.

Results

The binding of [^{3}H]SR141716A to WT and mutant receptors stably expressed in HEK 293 cells was measured to generate an estimate of the K_d and B_{max} values. Similar cell surface expression of WT and mutant cell lines was verified by immunofluorescence staining (unpublished data).

Radioligand Binding Assays

Saturation binding analysis of [^{3}H]SR141716A at the D2.63^{176}A, K373A, D2.63^{176}A-K373A, and D2.63^{176}K-K373D mutations displayed K_d (CL) values of 4.2 (0.1–9.8) nM, 1.7 (0.2–3.5) nM, 4.4 (0.1–9.1) nM, and 3.5 (0.1–24) nM, respectively (see Table 1). The K_d for the WT hCB_1 receptor was 2.2 (0.4–3.9) nM. The K_d values for the mutants versus WT were not statistically significantly different. Similarly, the B_{max} values for each cell line demonstrated that expression levels of these receptors between the different cell lines were comparable. The cell lines D2.63^{176}A, K373A, D2.63^{176}A-373A, and D2.63^{176}K-K373D respective B_{max} (CL) values were 2.3 (1.0–3.5) pmol/mg, 1.8 (0.1–3.7) pmol/mg, 2.7 (1.7–3.7) pmol/mg, and 0.7 (0.1–2.4) pmol/mg. The WT CB_1 cell line displayed a B_{max} of 2.4 (1.9–2.9) pmol/mg.

Competitive Binding Assays

We investigated the binding affinity of the bicyclic cannabinoid agonist CP55,940 to displace [^{3}H]SR141716A bound to the WT and mutant hCB_1 receptors. The K_i values between WT and mutant receptors overlapped and were not statistically significantly different (see Fig. 3; Table 2). The K_i (CL) values for WT, D2.63^{176}A, K373A, D2.63^{176}A-K373A, and

TABLE 1

Radioligand binding properties of wild-type and mutant cell lines

The K_d and B_{max} values were determined from saturation binding experiments using [^{3}H]SR141716A on HEK293 cell membrane preparations stably transfected with the wild-type or mutant hCB_1 receptor. Data represent the mean and corresponding S.E.M. of at least three independent experiments performed in triplicate. No statistically significant difference was observed between the wild-type and mutant binding properties as determined by a two-tailed Student's t test.

Radioligand	Cell Line	K_d (nM)	95% CL	B_{max}	95% CL
				pmol/mg	
[^{3}H]SR141716A	WT hCB_1	2.2	(0.4–3.9)	2.4	(1.9–2.9)
	D2.63^{176}A	4.2	(0.1–9.8)	2.3	(1.0–3.5)
	K373A	1.7	(0.2–3.5)	1.8	(0.1–3.7)
	D2.63^{176}A-K373A	4.4	(0.1–9.1)	2.7	(1.7–3.7)
	D2.63^{176}K-K373D	3.5	(0.1–24)	0.7	(0.1–2.4)

D2.63^{176}K-K373D were 17 (5.3–53) nM, 4.9 (0.6–43) nM, 17 (3.3–85) nM, 5.1 (0.63–42) nM, and 15 (3.0–69) nM, respectively.

Agonist Stimulated GTPγS Binding

We used [^{35}S]GTPγS binding to measure the stimulation of WT and mutant cannabinoid receptors upon stimulation with different classes of cannabinoid ligands (see Fig. 4; Table 3). The EC_{50} and E_{max} values were generated for WT and mutant receptor activation in the presence of CP55,940 and WIN55,212-2. The EC_{50} values of CP55,940 and WIN55,212-2 at WT CB_1 were 12.6 nM and 36.7 nM, respectively. The D2.63^{176}A mutation statistically significantly increased EC_{50} values for CP55,940 and WIN55,212-2 to 67 nM (5.3-fold) and 231 nM (6.3-fold), respectively, and the maximum agonist responsiveness was lower. The K373A mutation resulted in similar effects on the EC_{50} and E_{max} values. The K373A mutant generated a statistically significant increase in EC_{50} values from WT for CP55,940 and WIN55,212-2 to 70 nM (5.6-fold) and 274 nM (7.5-fold), respectively.

However, when the ionic interaction between D2.63^{176} and K373 was disrupted by double-alanine substitutions, the receptor activity was severely reduced. The D2.63^{176}A-K373A mutant resulted in dramatic shifts of either or both the EC_{50} and E_{max} values and for CP55,940 and WIN55,212-2 to 39.8 nM (E_{max} = 29%) and 561 nM (E_{max} = 59%), respectively. The largest shift observed was from WIN55,212-2, 15.3-fold above the WT value. In contrast, the charge-reversal mutant D2.63^{176}K-K373D displayed an EC_{50} and E_{max} for WIN55,212-2 of 126 nM and 79%, respectively. Likewise, the D2.63^{176}K-K373D mutant EC_{50} and E_{max} values for CP55,940 were 38 nM and 82%, respectively.

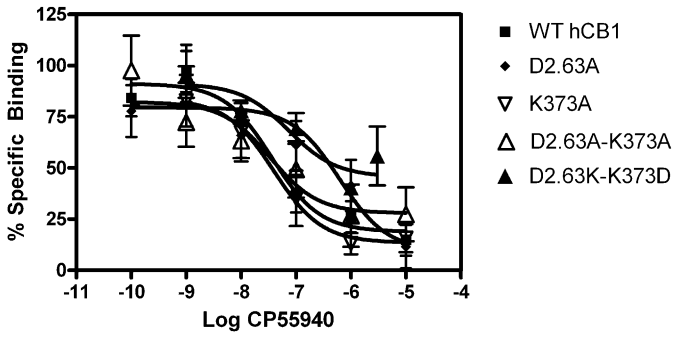

Fig. 3. Competitive displacement of [^{3}H]SR141716A. CP55,940 was used as the displacing compound. [^{3}H]SR141716A binding in membranes prepared from HEK293 cells stably transfected with wild-type, D2.63^{176}A, K373A, or D2.63^{176}A-K373A mutant CB_1 receptors. Each data point represents the mean ± S.E.M. of at least three independent experiments performed in triplicate.

Modeling Studies

Modeler Results: EC Loop Conformations in the WT CB_1 R* and the D2.63^{176}A, K373A, D2.63^{176}A-K373A, and D2.63^{176}K-K373D Mutants. As described in Materials and Methods, low-energy WT and mutant loop conformations were added to our previous CB_1 R* bundle (Kapur et al., 2007). Consistent with the experimental results, the WT model includes an ionic interaction between D2.63^{176} and EC-3 loop residue K373 (see Fig. 5). This ionic interaction causes the EC-3 loop to pull across the top (EC side) of the receptor. Clearly, this specific ionic interaction cannot form in the D2.63^{176}A, K373A, or the D2.63^{176}A-K373A mutant. By not forming this ionic interaction, the EC-3 loops of the mutant receptors experience greater conformational freedom. As illustrated in Fig. 5, the modeled loop conformations of D2.63^{176}A, K373A, and D2.63^{176}A-K373A position the EC-3 loop away from the center and are more directly above TMHs 6 and 7. It is noteworthy that these three mutants have very similar EC-3 loop conformations and that these conformations are fundamentally different from the WT EC-3 loop conformation.

Unlike the D2.63^{176}A, K373A, or the D2.63^{176}A-K373A mutant, the D2.63^{176}K-K373D swap mutant can form the putative ionic interaction. In agreement with the experimental results, the model of this mutant includes an ionic interaction between D2.63^{176}K and K373D (see Fig. 6). This ionic interaction causes the EC-3 loop to pull across the top (EC side) of the receptor. As observed in Fig. 6, the WT and the D2.63^{176}K-K373D EC loops have a remarkable degree of conformational similarity in their EC loops. The formation of

TABLE 2

The effects of amino acid mutations of recombinant hCB_1 receptors on the displacement of [^{3}H]SR141716A by CP55,940

Data represent the mean and corresponding 95% confidence limits of at least three independent experiments performed in triplicate. The K_i value of CP55,940 at the mutant receptors was not statistically significantly different from wild-type CB_1 receptors using a two-tailed Student's t test.

[^{3}H]SR141716A	CP 55,940 (K_i) + 95% CL
WT	17 nM (5.3–53)
D2.63^{176}A	4.9 nM (0.6–43)
K373A	17 nM (3.3–85)
D2.63^{176}A-K373A	5.1 nM (0.6–42)
D2.63^{176}K-K373D	15 nM (3.0–69)

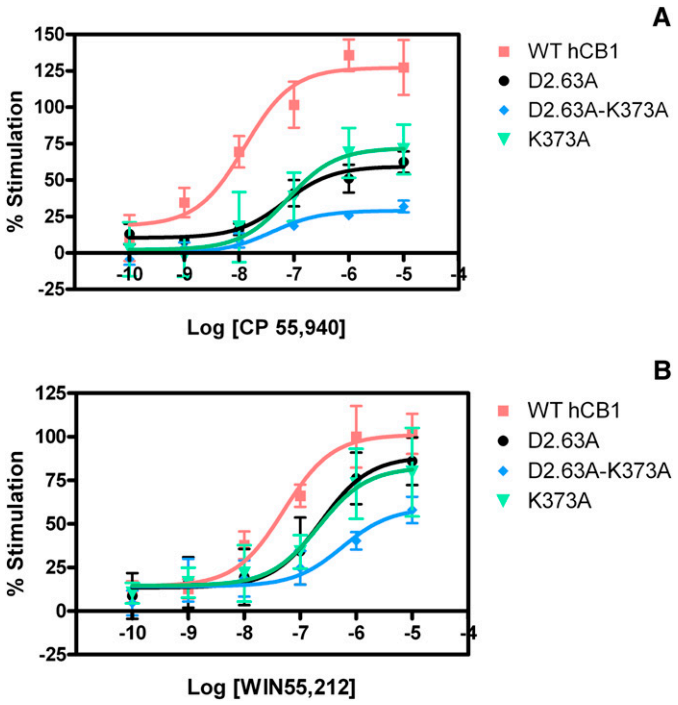

Fig. 4. Activation of wild-type and mutant receptors. (A) CP55,940. (B) WIN55,212-2. Concentration-effect curves were obtained from [^{35}S]GTPγS binding in HEK293 membrane preparations expressing wild-type or D2.63^{176}A, K373A, or D2.63^{176}A-K373A, D2.63^{176}K-K373D mutant CB_1 receptors. Each data point represents the mean ± S.E.M. of at least three independent experiments performed in triplicate.

the putative ionic interaction (despite having switched the residues at 2.63^{176} and 373) explains how the D2.63^{176}K-K373D swap mutant is capable of promoting an EC-3 loop conformation that is very similar to the WT EC-3 loop conformation.

In addition, the negatively charged K373D may be able to form ionic interactions with K370 and K7.32^{376} (see Fig. 1). These interactions may reduce the frequency of the D2.63^{176}K-K373D ionic interaction. Energetically favorable interactions with K370 and K7.32^{376} are highly unlikely for K373 (in WT), as its positive charge would be repelled by the positive charge on K370 and K7.32^{376}.

CP55,940/Receptor Pairwise and Total Interaction Energies. The results of the saturation and competitive binding assays demonstrate that all mutations do not significantly affect the binding affinity of the ligands studied. Therefore, to test whether our models agreed with these results, pairwise and total interaction energies were calculated for the WT and mutant models (the total interaction energies are listed in Table 4; the complete pairwise interaction energies are listed in Supplemental Tables 1–5). Only five residues contribute at least 5% of the total interaction energy between CP55,940 and each of the models (Supplemental Tables 1–5). Strikingly, these five important residues are the same in the WT and mutant models (Q1.32^{116}, F2.57^{170}, K3.28^{192}, S7.39^{383}, and L7.43^{387}). This consistency (in which residues contribute at least 5% of the total interaction energy) qualitatively suggests that CP55,940 binds WT and mutant receptors similarly. Quantitatively, Table 4 shows that none of the mutations resulted in significant change in the total interaction energy between CP55,940 and the receptor. These results indicate that our computational models are consistent with the results of the binding assays.

Discussion

In our present study, we have used computational methods together with model-guided mutagenesis to evaluate the functional importance of a putative intramolecular ionic interaction within the CB_1 receptor. Our previous mutation studies demonstrated the importance of a negative charge at residue 2.63^{176}, possibly indicating its involvement in an essential ionic interaction (Kapur et al., 2008). Our previous modeling studies indicated that the EC-3 loop residue K373 might be the ionic partner to D2.63^{176}. To test this hypothesis, four substitution mutant CB_1 receptors were constructed—D2.63^{176}A, K373A, D2.63^{176}A-K373A, and D2.63^{176}K-K373D—to evaluate the effect of removing the putative ionic interaction. The charge-reversal mutant was designed to determine whether switching the positions of the ionic partners could rescue WT levels of function. Finally, computational methods were also used to explore how the putative ionic interaction influences receptor structure.

TABLE 3

Concentration-effect data for agonist stimulation of [^{35}S]GTPγS binding of WT and mutant receptors stably expressed in HEK293 cells

Data represent the mean of at least three independent experiments performed in triplicate. EC_{50} values were determined from concentration-effect curves using GraphPad Prism software. The values in parentheses are 95% confidence intervals. Statistical analysis was performed by comparing the log EC_{50} of the mutant receptor to the wild-type CB_1 receptors using a two-tailed Student's t test to determine the level of significance.

	Drug	EC_{50} (95% CL)	E_{max}/Top (95% CL)	Mutant/WT EC_{50}
WT	CP55,940	12.6 nM (3.6–43.7)	127% (109–145)	NA
	WIN55,212-2	36.7 nM (12.4–108.3)	95% (87–116)	NA
D2.63^{176}A	CP55,940	67 nM (17–259)*	59% (48–71)*	5.3*
	WIN55,212-2	231 nM (27–1912)*	89% (60–118)	6.3*
K373A	CP55,940	70 nM (5.6–870)*	70% (44–100)	5.6*
	WIN55,212-2	274 nM (61–1230)*	83% (53–112)	7.5*
D2.63^{176}A-K373A	CP55,940	39.8 nM (10–153)*	29% (23–35)*	3.2*
	WIN55,212-2	561 nM (60–5193)*	59% (38–81)*	15.3*
D2.63K-K373D	CP55,940	38 nM (6.9–209)	82% (73–93)	3
	WIN55,212-2	126 nM (26–607)	79% (63–95)	3.4

*$P < 0.05$.

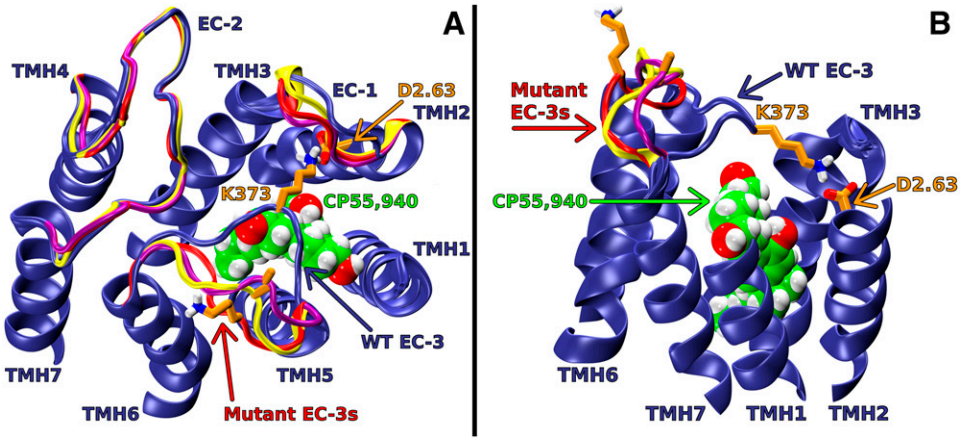

Fig. 5. Extracellular (EC) loop conformations of WT and D2.63^{176}A, K373A, or D2.63^{176}A-K373A mutant CB_1 receptors in the active (R*) state. CP55,940 is shown in green; D2.63^{176} and K373 are shown in orange; WT EC loops are shown in blue; D2.63^{176}A, K373A, and D2.63^{176}A-K373A mutant EC loops are shown in red, yellow, and purple, respectively. In the WT model, the putative ionic interaction between D2.63^{176} and K373 has formed; this promotes an EC-3 loop conformation that is pulled over the top of the receptor. In the alanine-substitution models, the putative interaction does not form, and the EC-3 loops are away from the bundle core. (A) Viewpoint is from EC with intracellular (IC) portions of TMHs, IC loops, and the N and C termini omitted to simplify view. (B) Viewpoint is from lipid looking between TMH1 and 7. Note: The IC portions of TMHs, IC loops, EC-1, EC-2, part of TMH1 and 7, and the N and C termini have been omitted here to simplify the view.

Ligand binding affinity was not significantly affected by any of the mutations performed here. These results are consistent with our prior characterization of D2.63^{176}, which was shown to be crucial for signal transduction but did not participate in high affinity agonist binding (Kapur et al., 2008). In addition, the binding affinity data reported here are consistent with the predictions made from our WT and mutant models. Specifically, CP55,940 was found to have a similar total interaction energy in the WT and mutant receptor models; this is not surprising, as neither D2.63^{176} nor the EC-3 loop are part of the predicted CP55,940 binding pocket. Indeed, reports of EC loop mutations that only affect agonist efficacy (and not ligand binding) are well documented in the GPCR literature. Residues in EC-2 loop of the M_3 muscarinic receptor could be mutated without affecting ligand binding; however, a significant reduction in agonist efficacy was observed (Scarselli et al., 2007). Similar results have been observed in the EC-1 loop of the adenosine A_{2B} receptor (Peeters et al., 2011a). Analogously, our results suggest that the ionic interaction between D2.63^{176} and K373 is not important for SR141716A (Table 1) or CP55,940 binding at the CB_1 receptor. Additionally, none of the mutations significantly affected the B_{max} for [^{3}H]SR141716A. These results suggest that the mutations reported here did not cause the receptor to fold incorrectly or fail to express at the cell surface.

In contrast to the binding affinity results, the D2.63^{176}A, K373A, D2.63^{176}A-K373A or D2.63^{176}K-K373D mutations caused a significant change in CP55,940s EC_{50} compared with WT. However, the EC_{50}s of the D2.63^{176}A, K373A, or the D2.63^{176}K-K373D mutants when compared with the D2.63^{176}A-K373A mutant were not significantly different. This is consistent with our hypothesis that it is the ionic interaction between the charged residues D2.63^{176} and K373 (and not the residues independently) that is important to agonist efficacy. If D2.63^{176} and K373 were independently important to function, one would expect that the EC_{50} of the double-alanine mutant would be higher than either of the single-alanine mutants.

We previously reported that presence of a negatively charged residue at position 2.63^{176} is crucial for receptor function (Kapur et al., 2008). In this study, we demonstrate that an ionic interaction between D2.63^{176} and K373 (not simply the negative charge on D2.63^{176} per se) is required for CB_1 WT function. The E_{max} values for either CP55,940 or

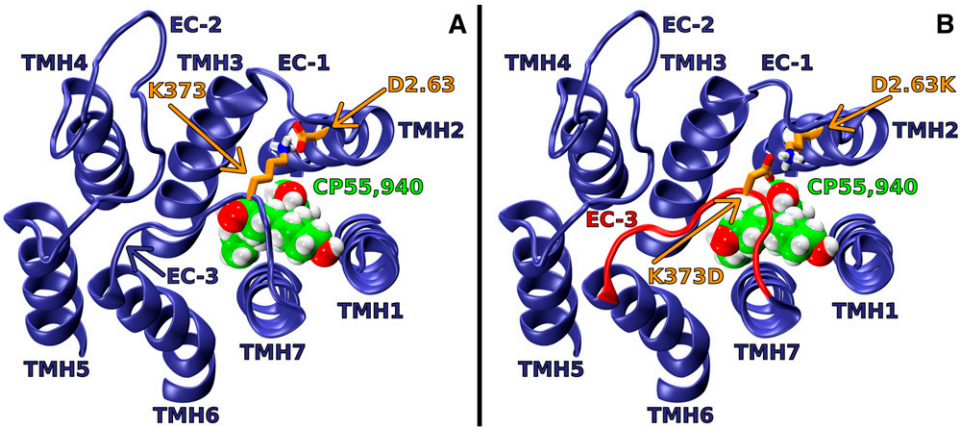

Fig. 6. Extracellular (EC) viewpoint of EC loop conformations of WT CB_1 R* and the D2.63^{176}K-K373D swap mutant. CP55,940 is shown in green; D2.63^{176} and K373 are shown in orange; WT EC loops are shown in blue; the D2.63^{176}K-K373D swap mutant EC-3 loop is shown in red (see Fig. 5 legend for further details). (A) In the WT model, the putative ionic interaction between D2.63^{176} and K373 has formed; this promotes an EC-3 loop conformation that is pulled over the top of the receptor. (B) In the D2.63^{176}K-K373D mutant model, the putative ionic interaction has been formed, promoting an EC-3 loop conformation that is very similar to WT.

TABLE 4
Total interaction energy of CP55,940 at the WT and mutant CB1 R* models

Model	Total Interaction Energies (kcal/mol)		
	Coulombic	VdW	Total
CB_1 WT	−22.12	−38.84	−60.95
D2.63^{176}A	−23.34	−36.94	−60.28
K373A	−23.34	−36.94	−60.28
D2.63^{176}A-K373A	−23.61	−38.60	−62.22
D2.63^{176}K-K373D	−24.72	−38.74	−63.46

WIN55,212-2 at the double-alanine mutant showed a significant decrease in function. This result suggests that the interaction between D2.63^{176} and K373 is important for signaling at CB_1. This result is also reinforced by results for the charge-reversal mutant D2.63^{176}K-K373D, as both CP55,940 and WIN55,212-2 showed a restoration of function compared with the double-alanine mutation. Therefore, the ability to switch the residues at 2.63^{176} and 373 (dramatically flipping the polarity on both residues) and preserve near WT levels of efficacy strongly supports the existence of a functionally required ionic interaction between D2.63^{176} and K373.

The single-alanine mutants showed increased E_{max} values relative to the double-alanine mutant (E_{max} = 59% at D2.63A and E_{max} = 29% for CP55,940; E_{max} = 89% at D2.63A and E_{max} = 59% for WIN55,212-2) that are larger than what might be expected for disruption of the same ionic interaction as seen in the double-alanine mutant. Our models suggest that residues near the putative ionic interaction may help rescue function in these single-alanine mutants. There are two additional lysines (K370 and K7.32^{376}, see Fig. 1) that are in close proximity to K373. These lysines may be able to form an ionic interaction with D2.63^{176}, thus partially rescuing function at the K373A mutant. Likewise, there is a negatively charged aspartate (D184) and two hydrophilic residues (H181 and D185) on the EC-1 loop that are in close proximity to D2.63^{176}. These residues may be able to form an ionic interaction (or a simple hydrogen bond in the case of H181 and S185) that enables the partial rescue of function at the D2.63^{176}A mutant. In the double mutant D2.63^{176}A-K373A, no such rescue would be possible because the polar residues at each site (D2.63 or K373) have been replaced with a nonpolar residue (Ala).

Involvement of EC Loops in GPCR Activation. Results reported here suggest that the formation of an ionic interaction/salt bridge between the EC-3 loop and the EC end of TMH2 is important for CB_1 signaling. The hallmark of class A GPCR activation by an agonist is the "tripping" of the toggle switch within the binding pocket that allows TMH6 to flex in the highly conserved Cys-Trp-any amino acid-Pro hinge region and straighten. This straightening breaks the "ionic lock" between R3.50 and E/D6.30 at the IC end of the receptor. The result is the formation of an IC opening of the receptor, exposing residues that can interact with the C terminus of the Gα-subunit of the G protein (Hamm et al., 1988). There is increasing evidence that movements in the EC loops also occur subsequent to agonist binding and are integral to transmission of the activation "message" (or covalent ligand isomerization in the case of rhodopsin). Nuclear magnetic resonance studies of rhodopsin activation by light have indicated that activation triggers a simultaneous displacement of the EC-2 loop and TMH5. Motion of EC-2 may allow the EC end of the TMH6-EC-3-TMH7 segment to pivot toward the center of the protein and conversely allow the IC end of TMH6 to rotate outward (Ahuja et al., 2009). In some class A GPCRs, such as chemokine receptor 4, a specific interaction between the EC-3 loop and N terminus (disulfide bridge) acts as a "microswitch" that is crucial to the chemokine receptor 4 signaling (Rana and Baranski, 2010).

The computational results reported here illustrate how the ionic interaction between D2.63^{176} and K373 causes the EC-3 loop to pull across the top (EC side) of the receptor. Notably, this EC-3 loop conformation is preserved in the charge-reversal mutant D2.63^{176}K-K373D. As described in *Results,* a strikingly different EC-3 loop conformation is observed in the three alanine-substitution mutants. These results suggest that the putative ionic interaction strongly influences the conformation of the EC-3 loop. This promoted EC-3 loop conformation could serve two important structural roles. First, this EC-3 loop conformation may contribute to forming a protected, closed EC surface, as has been reported in the crystal structures of rhodopsin (Li et al., 2004) and the sphingosine 1-phosphate receptor (Hanson et al., 2012). Second, this ionic interaction creates a noncovalent "tether" between the EC ends of TMHs 2, 6, and 7, allowing conformational changes that occur on one side of the receptor to be transmitted to the other side of the receptor. Thus, the alanine-substitution mutants are less capable of transmitting conformational changes throughout the receptor, and efficacy is consequently impaired. In conclusion, we have identified the EC-3 loop conformation that is mechanistically important in the signaling cascade in CB_1.

Acknowledgments

The authors thank Dr. Linda Console-Bram for comments on an earlier version of this manuscript.

Authorship Contributions

Participated in research design: Marcu, Abood, Shore, Makriyannis, Reggio, Kapur.

Conducted experiments: Marcu, Trznadel, Kapur, Shore.

Performed data analysis: Marcu, Kapur, Shore.

Wrote or contributed to the writing of the manuscript: Abood, Reggio, Shore, Marcu.

References

Ahn KH, Bertalovitz AC, Mierke DF, and Kendall DA (2009a) Dual role of the second extracellular loop of the cannabinoid receptor 1: ligand binding and receptor localization. *Mol Pharmacol* **76**:833–842.

Ahn KH, Pellegrini M, Tsomaia N, Yatawara AK, Kendall DA, and Mierke DF (2009b) Structural analysis of the human cannabinoid receptor one carboxyl-terminus identifies two amphipathic helices. *Biopolymers* **91**:565–573.

Ahuja S, Hornak V, Yan EC, Syrett N, Goncalves JA, Hirshfeld A, Ziliox M, Sakmar TP, Sheves M, and Reeves PJ, et al. (2009) Helix movement is coupled to displacement of the second extracellular loop in rhodopsin activation. *Nat Struct Mol Biol* **16**:168–175.

Andersson H, D'Antona AM, Kendall DA, Von Heijne G, and Chin CN (2003) Membrane assembly of the cannabinoid receptor 1: impact of a long N-terminal tail. *Mol Pharmacol* **64**:570–577.

Avlani VA, Gregory KJ, Morton CJ, Parker MW, Sexton PM, and Christopoulos A (2007) Critical role for the second extracellular loop in the binding of both orthosteric and allosteric G protein-coupled receptor ligands. *J Biol Chem* **282**: 25677–25686.

Ballesteros JA and Weinstein H (1995) Integrated methods for the construction of three dimensional models and computational probing of structure function relations in g protein-coupled receptors, in *Methods in Neuroscience* (Sealfon SC ed) pp 366–428, Academic Press, San Diego, CA.

Bertalovitz AC, Ahn KH, and Kendall DA (2010) Ligand binding sensitivity of the extracellular loop two of the cannabinoid receptor 1. *Drug Dev Res* **71**:404–411.

Bokoch MP, Zou Y, Rasmussen SG, Liu CW, Nygaard R, Rosenbaum DM, Fung JJ, Choi HJ, Thian FS, and Kobilka TS, et al. (2010) Ligand-specific regulation

of the extracellular surface of a G-protein-coupled receptor. *Nature* **463**: 108–112.
Bramblett RD, Panu AM, Ballesteros JA, and Reggio PH (1995) Construction of a 3D model of the cannabinoid CB1 receptor: determination of helix ends and helix orientation. *Life Sci* **56**:1971–1982.
Cheng YC and Prusoff WH (1973) Relationship between the inhibition constant (K1) and the concentration of inhibitor which causes 50 per cent inhibition (I50) of an enzymatic reaction. *Biochem Pharmacol* **22**:3099–3108.
Christopoulou FD and Kiortsis DN (2011) An overview of the metabolic effects of rimonabant in randomized controlled trials: potential for other cannabinoid 1 receptor blockers in obesity. *J Clin Pharm Ther* **36**:10–18.
Conner M, Hawtin SR, Simms J, Wootten D, Lawson Z, Conner AC, Parslow RA, and Wheatley M (2007) Systematic analysis of the entire second extracellular loop of the V(1a) vasopressin receptor: key residues, conserved throughout a G-protein-coupled receptor family, identified. *J Biol Chem* **282**:17405–17412.
Fay JF, Dunham TD, and Farrens DL (2005) Cysteine residues in the human cannabinoid receptor: only C257 and C264 are required for a functional receptor, and steric bulk at C386 impairs antagonist SR141716A binding. *Biochemistry* **44**: 8757–8769.
Fiser A, Do RK, and Sali A (2000) Modeling of loops in protein structures. *Protein Sci* **9**:1753–1773.
Hamm HE, Deretic D, Arendt A, Hargrave PA, Koenig B, and Hofmann KP (1988) Site of G protein binding to rhodopsin mapped with synthetic peptides from the alpha subunit. *Science* **241**:832–835.
Hanson MA, Roth CB, Jo E, Griffith MT, Scott FL, Reinhart G, Desale H, Clemons B, Cahalan SM, and Schuerer SC, et al. (2012) Crystal structure of a lipid G protein-coupled receptor. *Science* **335**:851–855.
Howlett AC, Barth F, Bonner TI, Cabral G, Casellas P, Devane WA, Felder CC, Herkenham M, Mackie K, and Martin BR, et al. (2002) International Union of Pharmacology. XXVII. Classification of cannabinoid receptors. *Pharmacol Rev* **54**: 161–202.
Jin W, Brown S, Roche JP, Hsieh C, Celver JP, Kovoor A, Chavkin C, and Mackie K (1999) Distinct domains of the CB1 cannabinoid receptor mediate desensitization and internalization. *J Neurosci* **19**:3773–3780.
Kapur A, Hurst DP, Fleischer D, Whitnell R, Thakur GA, Makriyannis A, Reggio PH, and Abood ME (2007) Mutation studies of Ser7.39 and Ser2.60 in the human CB1 cannabinoid receptor: evidence for a serine-induced bend in CB1 transmembrane helix 7. *Mol Pharmacol* **71**:1512–1524.
Kapur A, Samaniego P, Thakur GA, Makriyannis A, and Abood ME (2008) Mapping the structural requirements in the CB1 cannabinoid receptor transmembrane helix II for signal transduction. *J Pharmacol Exp Ther* **325**:341–348.
Li J, Edwards PC, Burghammer M, Villa C, and Schertler GF (2004) Structure of bovine rhodopsin in a trigonal crystal form. *J Mol Biol* **343**:1409–1438.
McAllister SD, Rizvi G, Anavi-Goffer S, Hurst DP, Barnett-Norris J, Lynch DL, Reggio PH, and Abood ME (2003) An aromatic microdomain at the cannabinoid CB (1) receptor constitutes an agonist/inverse agonist binding region. *J Med Chem* **46**: 5139–5152.
Murphy JW and Kendall DA (2003) Integrity of extracellular loop 1 of the human cannabinoid receptor 1 is critical for high-affinity binding of the ligand CP 55,940 but not SR 141716A. *Biochem Pharmacol* **65**:1623–1631.
Peeters MC, van Westen GJ, Guo D, Wisse LE, Müller CE, Beukers MW, and Ijzerman AP (2011a) GPCR structure and activation: an essential role for the first extracellular loop in activating the adenosine A2B receptor. *FASEB J* **25**:632–643.
Peeters MC, van Westen GJ, Li Q, and Ijzerman AP (2011b) Importance of the extracellular loops in G protein-coupled receptors for ligand recognition and receptor activation. *Trends Pharmacol Sci* **32**:35–42.
Pertwee RG (2009) Emerging strategies for exploiting cannabinoid receptor agonists as medicines. *Br J Pharmacol* **156**:397–411.
Picone RP, Fournier DJ, and Makriyannis A (2002) Ligand based structural studies of the CB1 cannabinoid receptor. *J Pept Res* **60**:348–356.
Rana S and Baranski TJ (2010) Third extracellular loop (EC3)-N terminus interaction is important for seven-transmembrane domain receptor function: implications for an activation microswitch region. *J Biol Chem* **285**:31472–31483.
Sali A and Blundell TL (1993) Comparative protein modelling by satisfaction of spatial restraints. *J Mol Biol* **234**:779–815.
Scarselli M, Li B, Kim SK, and Wess J (2007) Multiple residues in the second extracellular loop are critical for M3 muscarinic acetylcholine receptor activation. *J Biol Chem* **282**:7385–7396.
Sealfon SC, Chi L, Ebersole BJ, Rodic V, Zhang D, Ballesteros JA, and Weinstein H (1995) Related contribution of specific helix 2 and 7 residues to conformational activation of the serotonin 5-HT2A receptor. *J Biol Chem* **270**:16683–16688.
Straiker A, Wager-Miller J, and Mackie K (2012) The CB1 cannabinoid receptor C-terminus regulates receptor desensitization in autaptic hippocampal neurones. *Br J Pharmacol* **165**:2652–2659.
Tao Q and Abood ME (1998) Mutation of a highly conserved aspartate residue in the second transmembrane domain of the cannabinoid receptors, CB1 and CB2, disrupts G-protein coupling. *J Pharmacol Exp Ther* **298**:651–658.
Ulfers AL, McMurry JL, Kendall DA, and Mierke DF (2002) Structure of the third intracellular loop of the human cannabinoid 1 receptor. *Biochemistry* **41**: 11344–11350.
Xu H, Lu YF, Partilla JS, Zheng QX, Wang JB, Brine GA, Carroll FI, Rice KC, Chen KX, and Chi ZQ, et al. (1999) Opioid peptide receptor studies, 11: involvement of Tyr148, Trp318 and His319 of the rat mu-opioid receptor in binding of mu-selective ligands. *Synapse* **32**:23–28.
Zhou W, Flanagan C, Ballesteros JA, Konvicka K, Davidson JS, Weinstein H, Millar RP, and Sealfon SC (1994) A reciprocal mutation supports helix 2 and helix 7 proximity in the gonadotropin-releasing hormone receptor. *Mol Pharmacol* **45**: 165–170.

Address correspondence to: Mary E. Abood, Department of Anatomy and Cell Biology, Center for Substance Abuse Research, Temple University, Philadelphia, PA 19140. E-mail: mabood@temple.edu